Proceedings of the XII International Symposium on Dynamic Problems of Mechanics (DINAME 2007),
Varoto, P. S. and Trindade, M. A. (Editors), ABCM, Ilhabela, SP, Brazil, February 26 - March 2, 2007

Modeling and Experimental Identification of a Flexible Continuous Rotor

James Sanches Alves[1], Agenor de Toledo Fleury[2,3]

[1] CTMSP/Navy Technological Center at São Paulo

Av. Prof. Lineu Prestes, 2242 – Cidade Universitária

ZC05598-900, São Paulo, Brazil

e-mail: jamari@macbbs.com.br

[2] Mechanical Engineering Department, FEI University Center

Av. Humberto A. Castelo Branco, 3972 – Assunção

ZC09850-900, São Bernardo do Campo, Brazil

[3] Mechanical Engineering Department, Escola Politécnica da USP

Av. Prof. Mello Morais, 2231 – Cidade Universitária

05508-900, São Paulo, Brazil

e-mail: agfleury@fei.edu.br

Abstract: For several types of rotating machines, like turbo machinery and ultracentrifuges, rotor flexibility plays a significant role. In this work, a flexible continuous rotor model is proposed and the eigenfunction orthogonality relationships are achieved in order to generate a discrete model by means of the modal superposition principle. Rotor equations of motion are then derived with the modal superposition series truncated to an arbitrary number of vibration modes. A test rig, comprising a thin shaft and inertial disks, where two of these disks are magnetic actuators for identification test purposes, has been designed, manufactured and assembled. A numerical simulation model corresponding to the experimental apparatus has been generated taking into account the first six bending vibration modes. Simulation results allow getting the natural frequencies, eigenfunctions (backward and forward precessions) and the system frequency responses. The tests performed demonstrate very good agreement among theoretical and experimental results.

Keywords: Rotor dynamics, flexible continuous rotors, modal analysis.

INTRODUCTION

Flexible, high-speed rotors are found in several types of machines like turbomachinery and ultracentrifuges. Many of them have to pass through bending critical speeds to reach the nominal rotation. Rotor modeling is often performed by discrete methods like the finite element method or the transfer matrix method (Li et al., 2006). This paper develops a flexible continuous rotor model useful for balancing, unbalance response and active bearings control studies. A test rig is designed and constructed to experimentally simulate a rotor based in the continuous approach. Results show a very good agreement between expected and measured values (Alves, 2004).

The generic rotor model is composed by elements, with uniformly distributed inertia and stiffness parameters. These elements are assumed to have constant circular cross section and a constant mass density along their entire length and are referred as cylindrical elements. This modeling procedure takes into account translational and rotational inertia as well as gyroscope effects. The Bernoulli-Euler beam theory (no shear effects) is used to describe rotor element elastic deformations considering constant and isotropic material properties in its entire length. The point linking two adjacent elements is called a node, where parameters are concentrated and linear or flexural springs are assigned to simulate the stiffness of external bearings or the flexibility of internal couplings, respectively. Bearings may exhibit asymmetric stiffness values in two orthogonal axes of a given cross section but couplings are not allowed to. No damping, neither internal nor external, is considered. Only transversal bending vibrations are concerned here. Longitudinal and torsional vibrations are not taken into account.

Complex rotors can be modeled, in this way, like an assembly of several equivalent constant distributed parameter elements and nodes, with or without concentrated parameters, joining them. For example, a gear wheel mounted on a shaft, both made of different materials, can be modeled considering an equivalent mass density and equivalent inner and outer diameters for the cylindrical element inertia parameters calculations. In the same way, one should consider equivalent inner and outer diameters and equivalent Young modulus for the constant cross-sectional rigidity parameter calculation. If convenient, only the stiffness parameter due to the shaft should be taken into account. The feeling of the design engineer in assembling a rotor model like this is a key step in achieving good results.

Rotor Element Equations of Motion

The linearized set of equations of motion for a rotor element of length *dZ*, as shown in Fig. 1, in an inertial frame *XYZ*, according to Alves (2004), is given by:

$$\begin{aligned} m\frac{\partial^2 X(Z,t)}{\partial t^2} - j_t \frac{\partial}{\partial Z}\left(\frac{\partial^2}{\partial t^2}\left(\frac{\partial X(Z,t)}{\partial Z}\right)\right) - j_p \Omega \frac{\partial}{\partial Z}\left(\frac{\partial}{\partial t}\left(\frac{\partial Y(Z,t)}{\partial Z}\right)\right) + EI\frac{\partial^4 X(Z,t)}{\partial Z^4} &= f_X(Z,t) \\ m\frac{\partial^2 Y(Z,t)}{\partial t^2} - j_t \frac{\partial}{\partial Z}\left(\frac{\partial^2}{\partial t^2}\left(\frac{\partial Y(Z,t)}{\partial Z}\right)\right) + j_p \Omega \frac{\partial}{\partial Z}\left(\frac{\partial}{\partial t}\left(\frac{\partial X(Z,t)}{\partial Z}\right)\right) + EI\frac{\partial^4 Y(Z,t)}{\partial Z^4} &= f_Y(Z,t) \end{aligned} \tag{1}$$

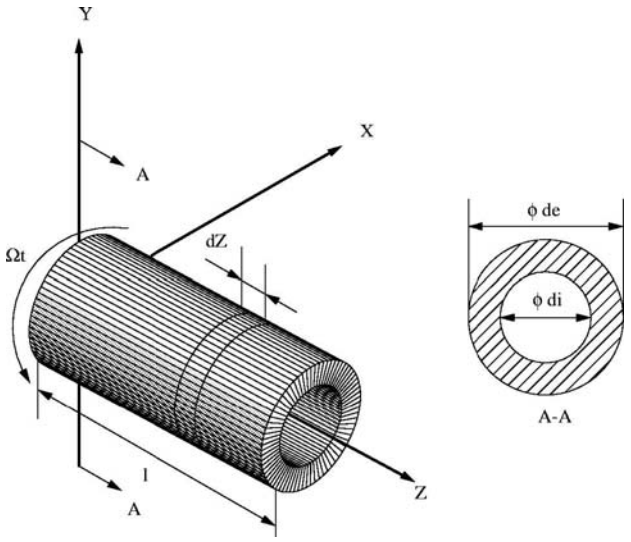

Figure 1 – Rotor element

where, m, j_t, j_p and EI, are the mass per unit length, the transversal mass moment of inertia of the cross section (equal for both *X* and *Y* axes), the polar mass moment of inertia of the cross section (with respect to *Z* axis) and the flexural rigidity, respectively. E is the Young's modulus of elasticity and I the cross-sectional area moment of inertia (equal with respect to X and Y axes). These parameters may be evaluated through the expressions (Alves, 2004):

$$m = \frac{M}{l} \text{ or } m = \rho\frac{\pi(d_e{}^2 - d_i{}^2)}{4};\ j_p = \frac{m(d_e{}^2 + d_i{}^2)}{8};\ j_t = \frac{j_p}{2};\ I = \frac{\pi(d_e{}^4 - d_i{}^4)}{64}$$

where, M, l, ρ, d_e and d_i are the total mass, the element length, the mass density, the outer and inner element diameters, respectively. All these parameters, as already mentioned, are assumed constant along the entire element length. Ω is the rotor angular velocity and $f_X(Z,t)$ and $f_Y(Z,t)$ are external transversal forces per unit length in the *X* and *Y* directions, respectively.

Substituting into the homogeneous part of Eq. (1), according to Pedersen (1972), synchronous solutions of the form:

$$\begin{aligned} X(Z,t) &= x_1(Z)\cos(\omega t) + x_2(Z)\sin(\omega t) \\ Y(Z,t) &= y_1(Z)\cos(\omega t) + y_2(Z)\sin(\omega t) \end{aligned} \tag{2}$$

The following eigenvalue problems arise:

$$\begin{aligned} m\omega^2 x_1 - j_t\omega^2 x_1'' + j_p\Omega\omega y_2'' - EIx_1{}^{IV} &= 0 \\ m\omega^2 y_2 - j_t\omega^2 y_2'' + j_p\Omega\omega x_1'' - EIy_2{}^{IV} &= 0 \end{aligned} \tag{3}$$

$$\begin{aligned} m\omega^2 x_2 - j_t\omega^2 x_2'' - j_p\Omega\omega y_1'' - EIx_2{}^{IV} = 0 \\ m\omega^2 y_1 - j_t\omega^2 y_1'' - j_p\Omega\omega x_2'' - EIy_1{}^{IV} = 0 \end{aligned} \tag{4}$$

From now on, dots denote differentiation with respect to time *t* and primes with respect to the length *Z*.

The corresponding natural boundary conditions are:

$$\begin{aligned} &T_{x_1} = -j_t\omega^2 x_1' + j_p\Omega\omega y_2' - EIx_1'''; T_{y_2} = -j_t\omega^2 y_2' + j_p\Omega\omega x_1' - EIy_2''' \\ &M_{x_1} = -EIy_2''; M_{y_2} = -EIx_1'' \end{aligned} \tag{5}$$

$$\begin{aligned} &T_{x_2} = -j_t\omega^2 x_2' - j_p\Omega\omega y_1' - EIx_2'''; T_{y_1} = -j_t\omega^2 y_1' - j_p\Omega\omega x_2' - EIy_1''' \\ &M_{x_2} = -EIy_1''; M_{y_1} = -EIx_2'' \end{aligned} \tag{6}$$

where, M is the bending moment and T is the shearing force.

The solutions for the above eigenvalue problems are given by (Parker and Sathe, 1999):

$$\begin{aligned} x_1 = {} & c1\cos(\beta_1 Z) + c2\sin(\beta_1 Z) + c3\cosh(\beta_3 Z) + c4\sinh(\beta_3 Z) + c5\cos(\beta_2 Z) + c6\sin(\beta_2 Z) + \\ & + c7\cosh(\beta_4 Z) + c8\sinh(\beta_4 Z) \end{aligned} \tag{7}$$

$$\begin{aligned} y_2 = {} & c1\cos(\beta_1 Z) + c2\sin(\beta_1 Z) + c3\cosh(\beta_3 Z) + c4\sinh(\beta_3 Z) - c5\cos(\beta_2 Z) - c6\sin(\beta_2 Z) - \\ & - c7\cosh(\beta_4 Z) - c8\sinh(\beta_4 Z) \end{aligned} \tag{8}$$

$$\begin{aligned} x_2 = {} & c9\cos(\beta_1 Z) + c10\sin(\beta_1 Z) + c11\cosh(\beta_3 Z) + c12\sinh(\beta_3 Z) + c13\cos(\beta_2 Z) + c14\sin(\beta_2 Z) + \\ & + c15\cosh(\beta_4 Z) + c16\sinh(\beta_4 Z) \end{aligned} \tag{9}$$

$$\begin{aligned} y_1 = {} & -c9\cos(\beta_1 Z) - c10\sin(\beta_1 Z) - c11\cosh(\beta_3 Z) - c12\sinh(\beta_3 Z) + c13\cos(\beta_2 Z) + c14\sin(\beta_2 Z) + \\ & + c15\cosh(\beta_4 Z) + c16\sinh(\beta_4 Z) \end{aligned} \tag{10}$$

with:

$$\begin{aligned} &\beta_1 = \sqrt{\frac{j_t\omega^2 - j_p\Omega\omega + \sqrt{4EI\mathrm{m}\omega^2 + (j_p\Omega\omega - j_t\omega^2)^2}}{2EI}}, \beta_2 = \sqrt{\frac{j_t\omega^2 + j_p\Omega\omega + \sqrt{4EI\mathrm{m}\omega^2 + (-j_p\Omega\omega - j_t\omega^2)^2}}{2EI}}, \\ &\beta_3 = \sqrt{\frac{-j_t\omega^2 + j_p\Omega\omega + \sqrt{4EI\mathrm{m}\omega^2 + (-j_p\Omega\omega + j_t\omega^2)^2}}{2EI}}, \beta_4 = \sqrt{\frac{-j_t\omega^2 - j_p\Omega\omega + \sqrt{4EI\mathrm{m}\omega^2 + (j_p\Omega\omega + j_t\omega^2)^2}}{2EI}} \end{aligned} \tag{11}$$

$x_1(Z)$, $x_2(Z)$, $y_1(Z)$ and $y_2(Z)$ are called eigenfunctions; β_1, β_2, β_3 and β_4 eigenvalues and ω is the natural frequency.

The constants $c1$, $c2 \ldots c16$ must be evaluated according to the boundary conditions which, besides the natural ones expressed by Eq. (5) and Eq. (6), are geometric (Meirovitch, 1977) and depend on the rotor elements constrains. Then, in order to determine these boundary conditions one must consider the rotor assembly.

Rotor Assembly

Figure (2) shows schematically the rotor assembly in the *OXZ* plane (similar procedure for the *OYZ* plane). As it can be seen, the rotor is composed by *n* elements. The *i-th* element has $l_i, m_i, j_{t_i}, j_{p_i}$ and EI_i constant parameters. The first and the last elements have free ends. There are *n-1* nodes. The *i-th* node has K_{X_i} and K_{Y_i} stiffness parameter of external linear springs in the *X* and *Y* directions, respectively. It has, also, F_i flexibility parameter of internal flexural spring equal in the *X* and *Y* directions.

The boundary conditions for each element shall be applied in the $O_i X_i Y_i Z$ local coordinate systems. Thus, the rotor element eigenfunctions will be derived in these local systems first. After that, the eigenfunctions of the whole rotor will be obtained in the *OXYZ* global coordinate system.

The linear springs forces are given by:

$$F_{X_i} = -K_{X_i} X_i(l_i) = -K_{X_i} X_{i+1}(0); F_{Y_i} = -K_{Y_i} Y_i(l_i) = -K_{Y_i} Y_{i+1}(0) \tag{12}$$

The moments in the flexural springs are:

$$M_{f_{X_i}}(l_i) = M_{f_{X_{i+1}}}(0) = -\frac{1}{F_i}(Y'_{i+1}(0) - Y'_i(l_i)); M_{f_{Y_i}}(l_i) = M_{f_{Y_{i+1}}}(0) = -\frac{1}{F_i}(X'_{i+1}(0) - X'_i(l_i)) \tag{13}$$

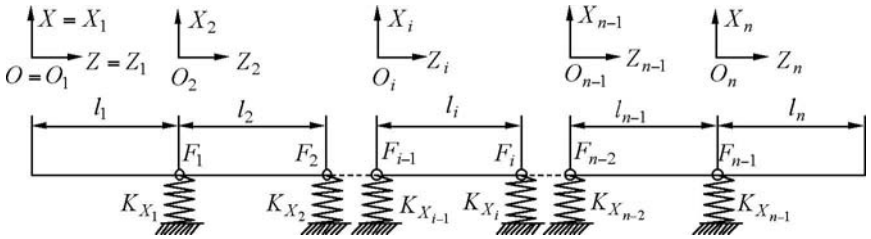

Figure 2 – Rotor assembly

To evaluate the constants $c1_i, c2_i, ..., c8_i$ of the eigenfunctions x_{1_i} and y_{2_i}, for each rotor element, the following boundary conditions must be applied:

For the first element:

$$M_{x_{1_1}}(0) = 0; M_{y_{2_1}}(0) = 0; T_{x_{1_1}}(0) = 0; T_{y_{2_1}}(0) = 0 \tag{14}$$

For the *n-th* element:

$$M_{x_{1_n}}(l_n) = 0; M_{y_{2_n}}(l_n) = 0; T_{x_{1_n}}(l_n) = 0; T_{y_{2_n}}(l_n) = 0 \tag{15}$$

For the *i-th* node:

$$\begin{aligned} &x_{1_{i+1}}(0) = x_{1_i}(l_i); y_{2_{i+1}}(0) = y_{2_i}(l_i); M_{x_{1_{i+1}}}(0) = -\frac{1}{F_i}(y'_{2i+1}(0) - y'_{2_i}(l_i)); M_{y_{2_{i+1}}}(0) = -\frac{1}{F_i}(x'_{1i+1}(0) - x'_{1_i}(l_i)); \\ &M_{x_{1_{i+1}}}(0) = M_{x_{1_i}}(l_i); M_{y_{2_{i+1}}}(0) = M_{y_{2_i}}(l_i);\ T_{x_{1_{i+1}}}(0) - T_{x_{1_i}}(l_i) = K_{x_i} x_{1_{i+1}}(0); T_{y_{2_{i+1}}}(0) - T_{y_{2_i}}(l_i) = K_{y_i} y_{2_{i+1}}(0) \end{aligned} \tag{16}$$

The eigenfuntions x_{1_i} and y_{2_i} are defined in local coordinate frames in the following domains:

$$\begin{aligned} x_{1_i} &= x_{1_i}(Z_i),\ \forall\ Z_i \in \Re\ \ni\ 0 \le Z_i \le l_i \\ y_{2_i} &= y_{2_i}(Z_i),\ \forall\ Z_i \in \Re\ \ni\ 0 \le Z_i \le l_i \end{aligned}$$

Substituting Eq. (5) on the $T_{x_{1_i}}$, $T_{y_{2_i}}$ shearing forces and $M_{x_{1_i}}$, $M_{y_{2_i}}$ bending moments, Eq. (7) and Eq. (8) of the x_{1_i} and y_{2_i} eigenfunctions, respectively and Eq. (11) of β_{1_i}, β_{2_i}, β_{3_i} and β_{4_i} eigenvalues into the boundary conditions given by Eqs. (14), (15) and (16), a set of equations takes place as follows:

$$\mathbf{A_s} \cdot \mathbf{C_s} = \mathbf{B_s} \tag{17}$$

where,

$$\begin{aligned} &\mathbf{A}_{\mathbf{s}_{8n\times 8n}}, \\ &\mathbf{C}_{\mathbf{s}_{8n\times 1}} = \left[c1_1\ \ .\ .\ c8_1\ \ .\ .\ c1_i\ \ .\ .\ c8_i\ \ .\ .\ c1_n\ \ .\ .\ c8_n\right]^t \quad i = 2,3,...n-1 \\ &\mathbf{B}_{\mathbf{s}_{8n\times 1}} = [0\ \ .\ .\ 0\ \ .\ .\ 0\ \ .\ .\ 0\ \ .\ .\ 0\ \ .\ .\ 0]^t \end{aligned}$$

The set of equations (17) possesses a nontrivial solution if and only if its characteristic determinant vanishes. The values of ω for which this condition is achieved are the so-called system natural frequencies. For each ω value, each element eigenvalues β_{1_i}, β_{2_i}, β_{3_i} and β_{4_i} can be evaluated by means of Eq. (11). Substituting a ω value in Eq. (17),

leads to the $c1_i, c2_i, ..., c8_i$ eigenfunctions constants, usually calculated assigning a value (unity, for instance) for one of the cj_i arbitrarily chosen. Substituting these constants into Eq. (7) and Eq. (8) one gets the x_{1_i} and y_{2_i} eigenfunctions.

Finally, in order to evaluate the whole rotor eigenfunctions corresponding to each natural frequency, according to Fig. (2), consider:

$$l_0 = 0$$
$$O_i = \sum_{j=1}^{i} l_{j-1}$$

where, O_i is the Z coordinate of the origin of the each element local $O_i X_i Y_i Z$ frame defined in the *OXYZ* global frame.

Defining the unit step function as being:

$$\mu(Z - O_i) = \begin{Bmatrix} 0 & for\ Z < O_i \\ 1 & for\ Z \geq O_i \end{Bmatrix}$$

The whole rotor eigenfunctions in the *OXYZ* global frame are given by:

$$x_1(Z) = \sum_{i=2}^{n+1} [\mu(Z - O_{i-1}) - \mu(Z - O_i)] \cdot x_{1_{i-1}}(Z - O_{i-1})$$
$$y_2(Z) = \sum_{i=2}^{n+1} [\mu(Z - O_{i-1}) - \mu(Z - O_i)] \cdot y_{2_{i-1}}(Z - O_{i-1})$$
$$\forall\ Z \in \Re\ \ni 0 \leq Z \leq l$$

where l is the rotor total length.

The same procedure must be used in determining the $x_2(Z)$ and the $y_1(Z)$ eigenfunctions. For each natural frequency the corresponding eigenfunctions give the so-called vibration mode.

Orthogonality Relationships

The two partial differential equations expressed by Eq. (1) can be rewritten as a set of first order differential equations as proposed by D'Eleuterio and Hughes (1984). To proceed so, the following operators are defined:

$$\mathbf{M} = \begin{bmatrix} m - j_t \dfrac{\partial^2}{\partial Z^2} & 0 \\ 0 & m - j_t \dfrac{\partial^2}{\partial Z^2} \end{bmatrix}, \mathbf{G} = \begin{bmatrix} 0 & -j_p \Omega \dfrac{\partial^2}{\partial Z^2} \\ j_p \Omega \dfrac{\partial^2}{\partial Z^2} & 0 \end{bmatrix}, \mathbf{K} = \begin{bmatrix} \mathrm{EI} \dfrac{\partial^4}{\partial Z^4} & 0 \\ 0 & EI \dfrac{\partial^4}{\partial Z^4} \end{bmatrix}$$

Substituting the above operators into Eq. (1) yields:

$$\mathbf{M}\ddot{\mathbf{d}} + \mathbf{G}\dot{\mathbf{d}} + \mathbf{K}\mathbf{d} = \mathbf{f_e} \tag{18}$$

where, $\mathbf{d} = \begin{bmatrix} X(Z,t) \\ Y(Z,t) \end{bmatrix}$ and $\mathbf{f_e} = \begin{bmatrix} f_x(Z,t) \\ f_y(Z,t) \end{bmatrix}$.

Eq. (18) is called a set of equations of motion in the configuration space.

Defining, yet, the operators:

$$\mathbf{E} = \begin{bmatrix} \mathbf{M} & \bullet \\ \bullet & \mathbf{K} \end{bmatrix}, \Gamma = \begin{bmatrix} \mathbf{G} & \mathbf{K} \\ -\mathbf{K} & \bullet \end{bmatrix}, \mathbf{r} = \begin{bmatrix} \dot{\mathbf{d}} \\ \mathbf{d} \end{bmatrix}, \Psi = \begin{bmatrix} \mathbf{f_e} \\ \bullet \end{bmatrix}$$

where, $(\bullet)$ is the order 2 column vector or square matrix null operator and substituting the above operators into Eq. (18) yields:

$$\mathbf{E}\dot{\mathbf{r}} + \Gamma\mathbf{r} = \Psi \tag{19}$$

Eq. (19) is called a set of equations of motion in the state space.

As it has already been seen, the solutions for the homogeneous part of Eq. (18) are given by the set Eq. (2). Taking the Eq. (2) time derivatives gives:

$$\begin{aligned}\dot{X}(Z,t) &= -\omega x_1(Z)\sin(\omega t) + \omega x_2(Z)\cos(\omega t)\\ \dot{Y}(Z,t) &= -\omega y_1(Z)\sin(\omega t) + \omega y_2(Z)\cos(\omega t)\end{aligned} \tag{20}$$

In the same way as for the Eq. (18), the homogeneous solutions of the set Eq. (19) may be written as follows:

$$\mathbf{r}(Z,t) = \mathbf{r_1}(Z)\cos(\omega t) + \mathbf{r_2}(Z)\sin(\omega t) \tag{21}$$

Substituting Eq. (2) into the configuration vector **d**, and, then, the resulting vector **d** and the set Eq. (20) into the state space vector **r** and, finally, this vector into Eq. (21), it is possible to get the following eigenfunctions in the state space:

$$\mathbf{r_1}(Z) = [\omega x_2(Z) \quad \omega y_2(Z) \quad x_1(Z) \quad y_1(Z)]^{\mathrm{t}}, \mathbf{r_2}(Z) = [-\omega x_1(Z) \quad -\omega y_1(Z) \quad x_2(Z) \quad y_2(Z)]^{\mathrm{t}} \tag{22}$$

For the *i-th* vibration mode with ω_i natural frequency, these eigenfunctions are given by:

$$\mathbf{r_{1}}_i(Z) = [\omega_i x_{2_i}(Z) \quad \omega_i y_{2_i}(Z) \quad x_{1_i}(Z) \quad y_{1_i}(Z)]^{\mathrm{t}}, \mathbf{r_{2}}_i(Z) = [-\omega_i x_{1_i}(Z) \quad -\omega_i y_{1_i}(Z) \quad x_{2_i}(Z) \quad y_{2_i}(Z)]^{\mathrm{t}} \tag{23}$$

Note that now the index *i* refers to the *i-th* vibration mode and not to the *i-th* rotor element.

Substituting Eq. (23) into Eq. (21) and the resulting vector into the homogeneous part of the set Eq. (19) the following eigenvalue problem in the state space results:

$$\begin{aligned}-\omega_i \mathbf{E}\mathbf{r}_{\mathbf{1}_i} + \Gamma \mathbf{r}_{\mathbf{2}_i} &= 0\\ \omega_i \mathbf{E}\mathbf{r}_{\mathbf{2}_i} + \Gamma \mathbf{r}_{\mathbf{1}_i} &= 0\end{aligned} \tag{24}$$

Now, multiply from the left the two equations in (24) by $\mathbf{r}_{\mathbf{1}_j}{}^{\mathrm{t}}$ and integrate each equation over the domain $0 \le Z \le l$.

Repeat this same procedure, multiplying from the left the two equations in (24) by $\mathbf{r}_{\mathbf{2}_j}{}^{\mathrm{t}}$, there resulting four equations.

For each equation, integral by parts are applied taking the boundary conditions of the whole rotor into account. After some tedious algebra manipulation, the following orthogonality relationships are achieved (Alves, 2004):

$$\omega_i\omega_j\int_0^l (\mathbf{v}_j{}^{\mathrm{t}}\mathbf{M}\mathbf{u}_i)dZ - \int_0^l (\mathbf{u}_j{}^{\mathrm{t}}\mathbf{K}\mathbf{v}_i)dZ = -\omega_i\omega_j\int_0^l (\mathbf{u}_j{}^{\mathrm{t}}\mathbf{M}\mathbf{v}_i)dZ + \int_0^l (\mathbf{v}_j{}^{\mathrm{t}}\mathbf{K}\mathbf{u}_i)dZ = 0$$

$$-\omega_i\int_0^l (\mathbf{u}_j{}^{\mathrm{t}}\mathbf{K}\mathbf{v}_i)dZ + \omega_i\omega_j\int_0^l (\mathbf{v}_j{}^{\mathrm{t}}\mathbf{G}\mathbf{v}_i)dZ + \omega_j\int_0^l (\mathbf{v}_j{}^{\mathrm{t}}\mathbf{K}\mathbf{u}_i)dZ = \omega_i\int_0^l (\mathbf{v}_j{}^{\mathrm{t}}\mathbf{K}\mathbf{u}_i)dZ + \omega_i\omega_j\int_0^l (\mathbf{u}_j{}^{\mathrm{t}}\mathbf{G}\mathbf{u}_i)dZ - \omega_j\int_0^l (\mathbf{u}_j{}^{\mathrm{t}}\mathbf{K}\mathbf{v}_i)dZ = 0$$

$$\omega_i\omega_j\int_0^l (\mathbf{u}_j{}^{\mathrm{t}}\mathbf{M}\mathbf{u}_i)dZ + \int_0^l (\mathbf{v}_j{}^{\mathrm{t}}\mathbf{K}\mathbf{v}_i)dZ = \omega_i\omega_j\int_0^l (\mathbf{v}_j{}^{\mathrm{t}}\mathbf{M}\mathbf{v}_i)dZ + \int_0^l (\mathbf{u}_j{}^{\mathrm{t}}\mathbf{K}\mathbf{u}_i)dZ = 2\omega_i{}^2\delta_{ij}$$

$$\omega_i\int_0^l (\mathbf{v}_j{}^{\mathrm{t}}\mathbf{K}\mathbf{v}_i)dZ + \omega_i\omega_j\int_0^l (\mathbf{u}_j{}^{\mathrm{t}}\mathbf{G}\mathbf{v}_i)dZ + \omega_j\int_0^l (\mathbf{u}_j{}^{\mathrm{t}}\mathbf{K}\mathbf{u}_i)dZ = 2\omega_i{}^3\delta_{ij}$$

$$\omega_i\int_0^l (\mathbf{u}_j{}^{\mathrm{t}}\mathbf{K}\mathbf{u}_i)dZ - \omega_i\omega_j\int_0^l (\mathbf{v}_j{}^{\mathrm{t}}\mathbf{G}\mathbf{u}_i)dZ + \omega_j\int_0^l (\mathbf{v}_j{}^{\mathrm{t}}\mathbf{K}\mathbf{v}_i)dZ = 2\omega_i{}^3\delta_{ij}$$

where, $\mathbf{u}_i = \begin{bmatrix} x_{1_i} \\ y_{1_i} \end{bmatrix}$, $\mathbf{v}_i = \begin{bmatrix} x_{2_i} \\ y_{2_i} \end{bmatrix}$, *j* refers to the *j-th* vibration mode and δ_{ij} is the Kronecker delta.

The integrals in the expressions above are inner products of the eigenfunctions and the **M**, **K** and **G** operators. Some of them, for the whole rotor, evaluated in local coordinate frames, are given bellow:

$$\int_0^l (\mathbf{v}_j{}^t \mathbf{M} \mathbf{v}_i) dZ = \sum_{k=1}^{n} [m_k (\int_0^{l_k} x_{2_{j,k}}(Z_k) x_{2_{i,k}}(Z_k) dZ + \int_0^{l_k} y_{2_{j,k}}(Z_k) y_{2_{i,k}}(Z_k) dZ) +$$
$$+ j_{t_k} (\int_0^{l_k} x'_{2_{j,k}}(Z_k) x'_{2_{i,k}}(Z_k) dZ + \int_0^{l_k} y'_{2_{j,k}}(Z_k) y'_{2_{i,k}}(Z_k) dZ)]$$

$$\int_0^l (\mathbf{u}_j{}^t \mathbf{K} \mathbf{u}_i) dZ = \sum_{k=1}^{n} [EI_k (\int_0^{l_k} x''_{1_{j,k}}(Z_k) x''_{1_{i,k}}(Z_k) dZ + \int_0^{l_k} y''_{1_{j,k}}(Z_k) y''_{1_{i,k}}(Z_k) dZ)] +$$
$$+ \sum_{k=1}^{n-1} [K_{X_k} x_{1_{j,k}}(l_k) x_{1_{i,k}}(l_k) + K_{Y_k} y_{1_{j,k}}(l_k) y_{1_{i,k}}(l_k) + F_k EI_k{}^2 x''_{1_{j,k}}(l_k) x''_{1_{i,k}}(l_k) + F_k EI_k{}^2 y''_{1_{j,k}}(l_k) y''_{1_{i,k}}(l_k)]$$

$$\int_0^l (\mathbf{v}_j{}^t \mathbf{G} \mathbf{u}_i) dZ = \sum_{k=1}^{n} [j_{p_k} \Omega (\int_0^{l_k} x'_{2_{j,k}}(Z_k) y'_{1_{i,k}}(Z_k) dZ - \int_0^{l_k} y'_{2_{j,k}}(Z_k) x'_{1_{i,k}}(Z_k) dZ)]$$

The index *k* refers to the *k-th* rotor element. As can be observed, the **M** and **K** operators are self-adjoint and the **G** operator is skew-self-adjoint. The other integrals have similar expressions.

Modal Discretization

The response of the system, according to the expansion theorem (Meirovitch, 1977), can be obtained by a superposition of the eigenfunctions multiplied by corresponding time-dependent generalized modal coordinates as follows:

$$\mathbf{r}(Z,t) = \sum_{i=1}^{\infty} [\mathbf{r}_{\mathbf{1}_i}(Z) \eta_{1_i}(t) + \mathbf{r}_{\mathbf{2}_i}(Z) \eta_{2_i}(t)] \tag{25}$$

where, $\eta_{1_i}(t)$ and $\eta_{2_i}(t)$ are generalized modal coordinates for the *i-th* vibration mode.

Substituting Eq. (25) into Eq. (19) yields:

$$\sum_{i=1}^{\infty} [\dot{\eta}_{1_i}(t) \mathbf{E} \mathbf{r}_{\mathbf{1}_i}(Z) + \dot{\eta}_{2_i}(t) \mathbf{E} \mathbf{r}_{\mathbf{2}_i}(Z)] + \sum_{i=1}^{\infty} [\eta_{1_i}(t) \Gamma \mathbf{r}_{\mathbf{1}_i}(Z) + \eta_{2_i}(t) \Gamma \mathbf{r}_{\mathbf{2}_i}(Z)] = \Psi \tag{26}$$

Multiplying Eq. (26) by $\mathbf{r}_{\mathbf{1}_j}{}^t$ from the left and integrating it over the domain $0 \le Z \le l$ and repeating the same procedure, but multiplying Eq. (26) by $\mathbf{r}_{\mathbf{2}_j}{}^t$, two equations arise. Introducing the orthogonality relationships in each of them, the following equations of motion for each *i-th* vibration mode are obtained:

$$\begin{aligned} \dot{\eta}_{1_i} + \omega_i \eta_{2_i} &= \frac{1}{2\omega_i} \int_0^l (\mathbf{v}_i{}^t \mathbf{f}_\mathbf{e}) dZ \\ \dot{\eta}_{2_i} - \omega_i \eta_{1_i} &= -\frac{1}{2\omega_i} \int_0^l (\mathbf{u}_i{}^t \mathbf{f}_\mathbf{e}) dZ \end{aligned} \tag{27}$$

Although no damping has been used in this model development up to now, a small modal viscous damping factor ξ_i can be added to the set Eq. (27). This can be done since usually ξ_i <<<1 and a small damping doesn't change significantly the natural frequencies and the corresponding eigenfunctions, which were previously evaluated considering the rotor-bearings system with no damping. With the added modal damping factors, the Eq. (27) becomes:

$$\begin{aligned} \dot{\eta}_{1_i} + \xi_i \omega_i \eta_{1_i} + \omega_i \eta_{2_i} &= \frac{1}{2\omega_i} \int_0^l (\mathbf{v}_i{}^t \mathbf{f}_\mathbf{e}) dZ \\ \dot{\eta}_{2_i} + \xi_i \omega_i \eta_{2_i} - \omega_i \eta_{1_i} &= -\frac{1}{2\omega_i} \int_0^l (\mathbf{u}_i{}^t \mathbf{f}_\mathbf{e}) dZ \end{aligned} \tag{28}$$

The displacement system output will be given by:

$$\mathbf{d}(Z,t) = \sum_{i=1}^{\infty} [\mathbf{u}_i(Z) \eta_{1_i}(t) + \mathbf{v}_i(Z) \eta_{2_i}(t)] \tag{29}$$

Numerical Simulations

Figure 3 shows the rotor test rig that has been designed and built to experimentally simulate a flexible rotor modeled using the above procedure (Alves, 2004).

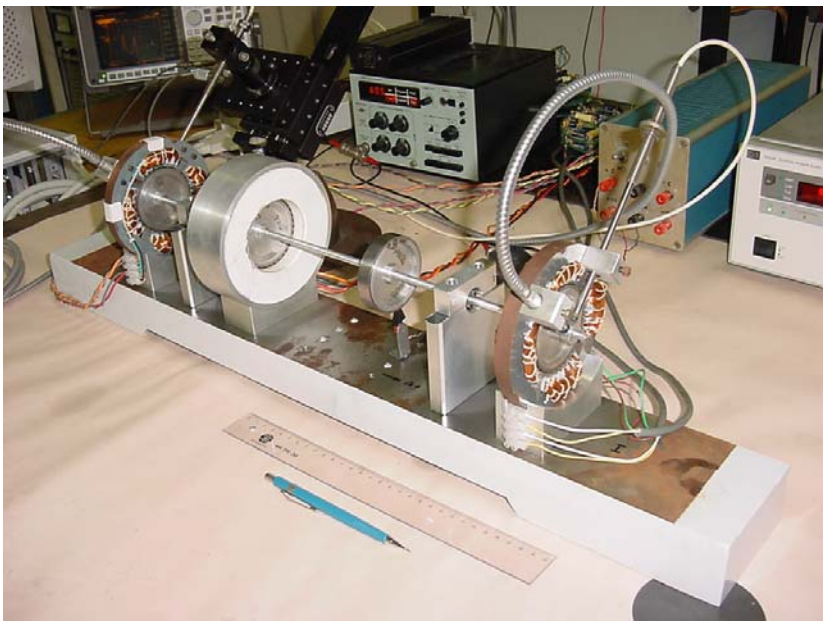

Figure 3 - Rotor test rig

The rotor is composed by a very flexible shaft and four disks supported by two self-compensating ball bearings. The two end disks are rotors of magnetic actuators that provide magnetic actuating forces in two orthogonal directions (*X* and *Y*) for each disk. The second disk (from left to right) is the rotor of a histheresis motor. The third disk is equal to the other ones and has an optical mark that can be read by a key-phasor sensor. Adjacent to the end disks, there are rings, which displacements can be measured by eddy current based displacement transducers in two orthogonal directions, either.

This rotor has been modeled as shown in the schematic Fig. 4:

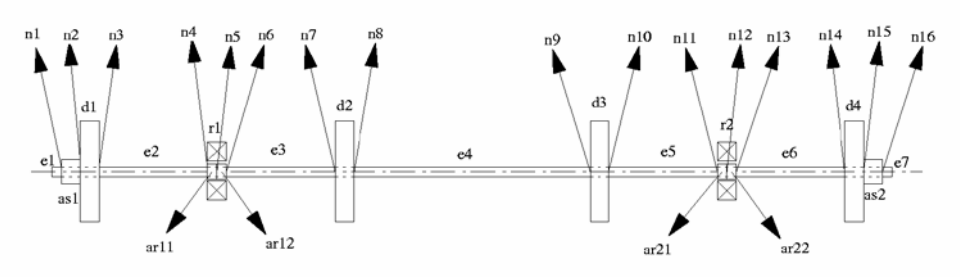

Figure 4 - Schematic test rig rotor model

The model comprises seventeen rotor elements. Seven of them are shaft elements (e1...e7), four are disk elements (d1...d4), four are ball bearing inner ring elements (ar11, ar12, ar21, ar22) and two are displacement sensor rings (as1, as2). There are sixteen nodes (n1...n16). In nodes n5 and n12 high stiffness linear springs are assigned in order to simulate the bearings stiffness. For disk and ring elements the inertia parameters are considered as the sum of the disks or rings plus the shaft inertia parameters. On the other hand, the flexural rigidity is due to the shaft, alone.

In order to achieve the natural frequencies and the corresponding eigenfunctions, a computer script has been developed using MATLAB™ software. This script employs a characteristic determinant root finder using the *regula falsi* algorithm. Figure 5 shows the natural frequencies and the normalized eigenfunctions for the third and the fourth vibration modes at the rotational speed of 20 Hz:

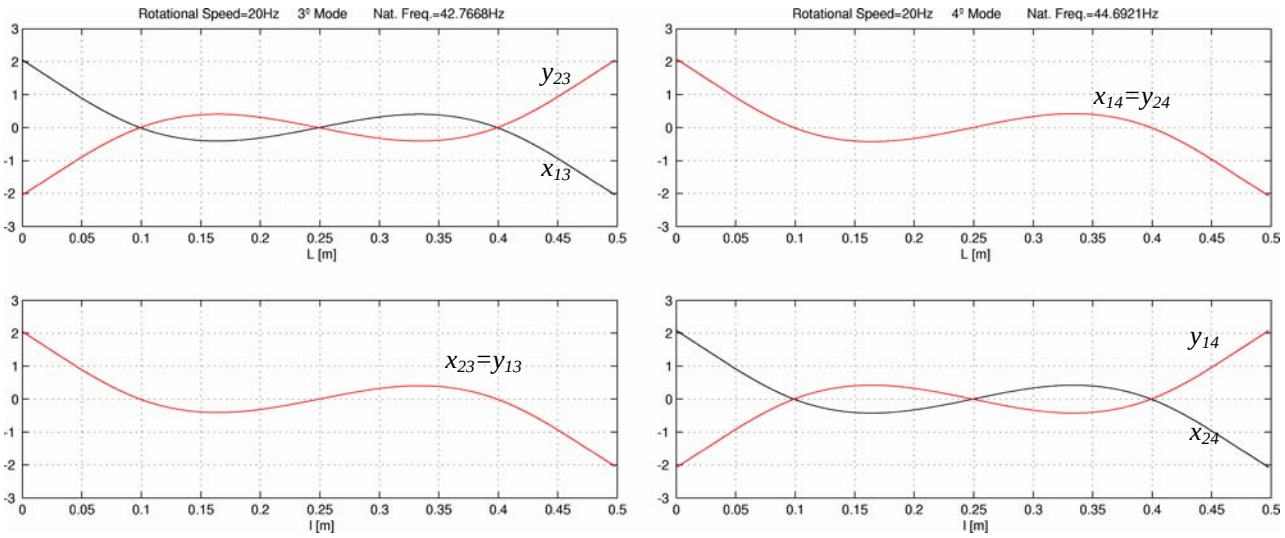

Figure 5 - Eigenfunctions for the 3º and 4º modes at the speed of 20 Hz

The third mode corresponds to a backward precession and the fourth one to a forward precession.

Analytical and Experimental Frequency Response Functions

In order to evaluate the analytical frequency response function (FRF), the rotor-bearing system matrices are assembled in state space form up to the sixth vibration mode, as follows:

$$\begin{aligned} \dot{\eta} &= \mathbf{A}\eta + \mathbf{B}\mathbf{u} \\ \mathbf{d} &= \mathbf{C}\eta \end{aligned} \tag{30}$$

where, $\eta = [\eta_{1_1} \quad \eta_{2_1} \quad \eta_{1_2} \quad \eta_{2_2} \quad \eta_{1_3} \quad \eta_{2_3} \quad \eta_{1_4} \quad \eta_{2_4} \quad \eta_{1_5} \quad \eta_{2_5} \quad \eta_{1_6} \quad \eta_{2_6}]^t$ are the modal generalized coordinates from the first to the sixth modes, $\mathbf{d} = [Y_{as1}]$ is the displacement in the *Y* direction of the ring as1 adjacent to the disk d1 which is the FRF output that has been used in the test identification procedure and is placed in the G_{as1} position on the *Z* axis (middle of the ring, see Fig. 4). In this test, $\mathbf{f_e} = [FY_{d1}\delta(Z - G_{d1})]$ is the FRF input which is the punctual magnetic actuating force in the *Y* direction applied in the disk d1 in the G_{d1} position on the *Z* axis (middle of the disk).

By introducing Eq. (28) and (29) into the Eq. (30), the system matrices result:

$$\mathbf{A} = \begin{bmatrix} -\xi\omega_1 & -\omega_1 & 0 & 0 & 0 & 0 \\ \omega_1 & -\xi\omega_1 & 0 & 0 & 0 & 0 \\ 0 & 0 & . & . & 0 & 0 \\ 0 & 0 & . & . & 0 & 0 \\ 0 & 0 & 0 & 0 & -\xi\omega_6 & -\omega_6 \\ 0 & 0 & 0 & 0 & \omega_6 & -\xi\omega_6 \end{bmatrix} \quad \mathbf{B} = \begin{bmatrix} \dfrac{y_{2_1}(G_{d1})}{2\omega_1} \\ -\dfrac{y_{1_1}(G_{d1})}{2\omega_1} \\ . \\ . \\ \dfrac{y_{2_6}(G_{d1})}{2\omega_6} \\ -\dfrac{y_{1_6}(G_{d1})}{2\omega_6} \end{bmatrix}$$

$$\mathbf{C} = [y_{1_1}(G_{as1}) \quad y_{2_1}(G_{as1}) \quad . \quad . \quad y_{1_6}(G_{as1}) \quad y_{2_6}(G_{as1})]$$

$$\mathbf{U} = [FY_{d1}].$$

Analytical FRF's have been obtained with the *freqresp* MATLAB™ command for the rotor immobile and for a rotational speed of 20 Hz. A modal damping factor $\xi = 5 \times 10^{-3}$ was adopted for all modes.

The experimental FRF's have been obtained using the HP™ 3567A signal analyzer. This equipment has a source signal generator (in voltage) that is sent to a power amplifier, which converts it in an electrical current that is converted to a magnetic force on the magnetic actuator of the disk d1 (Alves et al., 1996). This signal may be a swept sine (used on the immobile rotor FRF) or a random noise filtered in a certain frequency bandwidth (used on the rotor at speed of 20 Hz FRF). The source signal is sent to an input channel on the analyzer and the displacement sensor signal of the as1 ring is sent to another channel. The analyzer performs the sinusoidal transfer function between the sensor and the source signals. In the case of the random noise source, measure data average is performed in the frequency domain. Obviously, the gains of the displacement sensor, power amplifier and the magnetic actuator must be taken into account.

Figure 6 shows the comparison between the analytical and the experimental FRF's obtained with the rotor immobile and at a rotating speed of 20 Hz. As it can bee seen, there is very good agreement among the analytical and the experimental results.

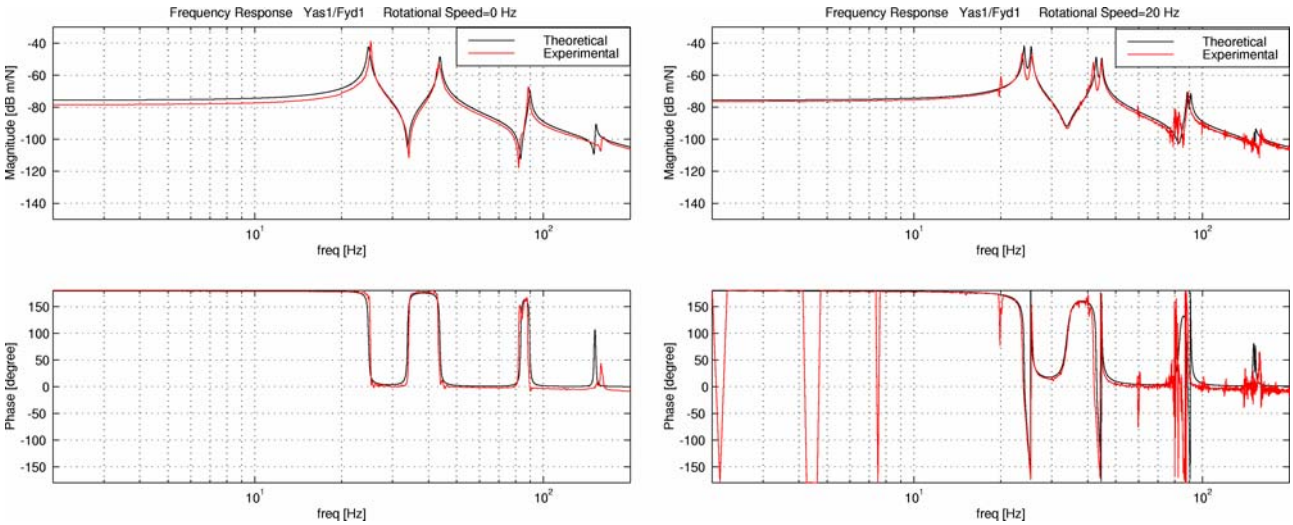

Figure 6 - Comparison between analytical and experimental FRF's

Conclusions

A flexible continuous rotor model has been obtained successfully. New eigenfunction orthogonality relationships for this case have been achieved, allowing modal discretization by means of the modal superposition principle. This feature makes this rotor model quite useful for balancing, unbalance response and active bearings control studies because, despite its computational cost in obtaining the natural frequencies and eigenfunctions, it can generate an accurate low order model considering only the vibration modes of interest. A test rig has been designed, manufactured and assembled. A numerical simulation model corresponding to the experimental apparatus has been generated taking into account the first six bending vibration modes allowing to get the natural frequencies, eigenfunctions (backward and forward precessions) and the system frequency responses. The tests performed, represented by some experimental rotor FRF's generated with the aid of the test rig magnetic actuator working like a non-contact shaker, demonstrate very good agreement between the theoretical and the experimental results.

ACKNOWLEDGEMENTS

The authors would like to thank Eng. Sidney Ricardo Alvarez Junior who had the first ideas concerning this rotor modeling approach and all colleagues from the CTMSP for their support in the experimental part of this work. The second author would like also to gratefully acknowledge CNPq for financial support.

REFERENCES

Alves, J. S., 2004, "Otimização Teórico-Experimental da Passagem por Velocidades Críticas de um Rotor Flexível Contínuo", Master Degree Dissertation, Politécnica School, University of São Paulo, São Paulo, Brazil 136 p.

Alves, J. S., Betti, F., Pierri, P. S. and Porsch, M. C., 1996, "Sistemas de Controle para Mancais Magnéticos Ativos", Proceedings of the I Symposium of Applied Automatics, Automatics Brazilian Society, São Paulo, Brazil, pp.135-140.

D'Eleuterio, G.M.T. and Hughes, P.C., 1984, "Dynamics of Gyroelastic Continua", Journal of Applied Mechanics, Transactions of the ASME, Vol. 51, pp. 415- 422.

Li, G., Lin, Z., Allaire, P. E., Luo, J., 2006, "Modeling of a High Speed Rotor Test Rig With Active Magnetic Bearings", Journal of Vibration and Acoustics, Transactions of the ASME, Vol. 128 , pp. 269-281.

Meirovitch, L., 1977, "Elements of Vibration Analysis**",** International Student Edition, McGraw-Hill Inc.

Parker, R.G. and Sathe, P.J., 1999, "Exact Solutions for the Free and Forced Vibration of a Rotating Disk-Spindle System", Journal of Sound and Vibration, Academic Press, Vol. 223, pp. 445-465.

Pedersen, P.T., 1972, "On Forward and Backward Precession of Rotors", Ingenieur Archiv**,** Springer-Verlag, Vol. 42, pp. 26- 41.

RESPONSIBILITY NOTICE

The authors are the only responsible for the printed material included in this paper.